KSCE Journal of Civil Engineering (2020) 24(11):3267-3278
DOI 10.1007/s12205-020-0572-6

pISSN 1226-7988, eISSN 1976-3808
www.springer.com/12205

Geotechnical Engineering

# Investigation on Mechanical and AE Characteristics of Yellow Sandstone Undergoing Wetting-Drying Cycles

**Yaoyao Meng[a], Hongwen Jing[a], Qian Yin[a], and Xiaowei Gu[a]**

[a]*State Key Laboratory for Geomechanics and Deep Underground Engineering, China University of Mining and Technology, Xuzhou 221116, China*

**ARTICLE HISTORY**

Received March 28, 2020
Revised May 30, 2020
Accepted June 26, 2020
Published Online 10 September 2020

**KEYWORDS**

Sandstone
Wetting-drying cycles
Mechanical properties
AE characteristics
Loading rate

**ABSTRACT**

The cyclic wetting-drying phenomenon is a complicated physical and chemical process. This kind of process will weaken the properties of rock to some extent. Some fundamental physical parameters of sandstone were first tested to study the weakening influence of wetting-drying cycles on the physical characteristics. Then, the water weakening effect on the mechanical and acoustic emission (AE) characteristics of rock on account of wetting-drying cycles was experimentally studied. Laboratory test results showed that when the number of cycles increased from 0 to 25, the density, *P*-wave velocity, uniaxial compressive strength (UCS), (elastic modulus (E)) and total AE counts of the rock specimens continuously decreased. However, the water absorption would increase as the number of cycles increased. The functional relationships between the total AE counts and the mechanical parameters (UCS and *E*) of sandstone after each cyclic number were established based on the test results. In addition, the chemical components and microstructure variations of rock undergoing wetting-drying cycles were examined. From the results, it can be concluded that microcrack growth and expansion inside the rocks undergoing wetting-drying cycles are the main reasons for the attenuation of the rock properties. Moreover, with increasing loading rate, the UCS, *E* and total AE counts of sandstone after each cyclic number would increase.

## 1. Introduction

Rock masses in actual engineering applications are periodically subjected to moist conditions. In these rock engineering applications, the rock's deterioration is closely related to the presence of water. The actions of wetting-drying cycles on the rock can be initiated by daily, seasonal and even yearly variations in the rainfall, humidity, and underground water level. These actions can accelerate the weathering process of rock. The water in the rock can also cause crack initiation, propagation, and coalescence, which may further accelerate the damage of rock (Zhou et al., 2018b; Zhou et al., 2019; Zhou and Zhuang, 2020; Zhou et al., 2020; Zhuang et al., 2020). Finally, many geological hazards, such as deformation of the building foundation, pillar degradation and landslides can occur over the time. Therefore, studying the wetting-drying cycle attenuation of the physical and mechanical characteristics of rock is of important significance.

In the last few years, scholars have focused on the weakening influence of wetting-drying cycles on the physical and mechanical characteristics of various kinds of rocks. Rock deterioration after wetting-drying cycles is often evaluated by variations in many physical parameters including the water absorption, weight loss, density, porosity, and *P*-wave velocity (Özbek, 2014; Zhao et al., 2018; Zhou et al., 2018a). In terms of mechanical characteristics, Khanlari and Abdilor (2015) studied the effect of wetting-drying cycles on the UCS of five kinds of sandstones. The test results showed that the smallest and greatest decreases in the UCS after 40 wetting-drying cycles were 11% and 21%, respectively. Liu et al. (2018) researched the strength variations of shaly sandstone undergoing different numbers of wetting-drying cycles. The experimental data indicated that with increasing cyclic wetting-drying, the UCS and *E* would markedly decrease. Qin et al. (2018) studied the mechanical parameters of pit rock after wetting-drying cycles. The results presented that with increasing cyclic wetting-drying, UCS and *E* decreased. The relations between the mechanical parameters (UCS and *E*) and the number

**CORRESPONDENCE** Hongwen Jing hongwenjingcumt@163.com State Key Laboratory for Geomechanics and Deep Underground Engineering, China University of Mining and Technology, Xuzhou 221116, China

ⓒ 2020 Korean Society of Civil Engineers

of cyclic wetting-drying were described by an exponential function. In addition to uniaxial compression test, other mechanical parameters of rock including the rebound value (Liu et al., 2016), tensile strength (Zhao et al., 2017; Sun and Zhang, 2019), shear behavior (Zhang et al., 2015; Wang et al., 2019), triaxial properties (Deng et al., 2012; Zhang et al., 2014) and fracture toughness (Hua et al., 2015; Hua et al., 2016) have also been investigated by researchers.

Acoustic emission (AE) is a common physical phenomenon and non-destructive test method. Owing to the advantages of its low cost, non-destruction and high efficiency, AE technology has been widely used by many scholars to study crack formation, crack expansion and rock damage during rock mechanics tests (Cai et al., 2019; Gong et al., 2019; Liu et al., 2020). During uniaxial compression, Lei et al. (2019) used AE energy as the main parameter to study the AE characteristics of sandstone after different temperatures treatment. The results indicated that as the temperature increased, the maximum AE energy firstly increased and then decreased. Kim et al. (2015) used AE and stress-strain methods to quantitatively assess the damage of granite. The damage factors derived from the AE energy and stress-strain relationship were both compared and analyzed. In terms of field applications and the accuracy of damage values, the AE energy method is superior to the stress-strain method. During the three-point bending tests, the AE monitoring system was used by Backers et al. (2005) to study the loading rate effect. The results indicated that accumulated AE events would increase with increasing loading rate. However, there are still limited studies on the AE characteristics of rock after wetting-drying cycles. In particular, the relationship between the AE parameters and mechanical parameters of rock after wetting-drying cycles has not been studied thus far. In fact, AE technology as a non-destructive test method can be used in field tests to reflect the mechanical conditions of the rock mass. Therefore, the investigation on the mechanical and AE characteristics of rock after wetting-drying cycles is of great importance to ensure the safety and stability of actual engineering applications.

The research objectives are to understand the attenuation mechanism in rock undergoing wetting-drying cycles and the effect on the mechanical and AE parameters of rocks. In this study, the chemical components and microstructure variations of sandstone were observed to obtain the attenuation mechanism in rocks undergoing wetting-drying cycles. The uniaxial compression test and AE test were conducted to study the variations in the mechanical and AE parameters of sandstone undergoing different cyclic numbers. The relationship between the mechanical and AE parameters of sandstone undergoing wetting-drying cycles was analyzed and established. In addition, the effect of the loading rate on the mechanical and AE characteristics was also studied.

## 2. Experiment

### 2.1 Specimen Preparation

In this experiment, the yellow sandstone studied in this paper is selected from Linyi City. The content of the sand grains in the diameter range of 0.05 mm to 0.25 mm is more than 50%. Therefore, the rock type is a fined-grained yellow sandstone. The mineralogical compositions are determined by X-ray diffraction (XRD). Fig. 1 shows that the mineral compositions of the sandstone are mainly quartz, kaolinite and clinochlore. The specimens used in this test are all drilled from the same block. According to the International Society for Rock Mechanics (ISRM) standards, the specimens are cut into cylinders with dimensions of Φ50 × 100 mm (diameter × height).

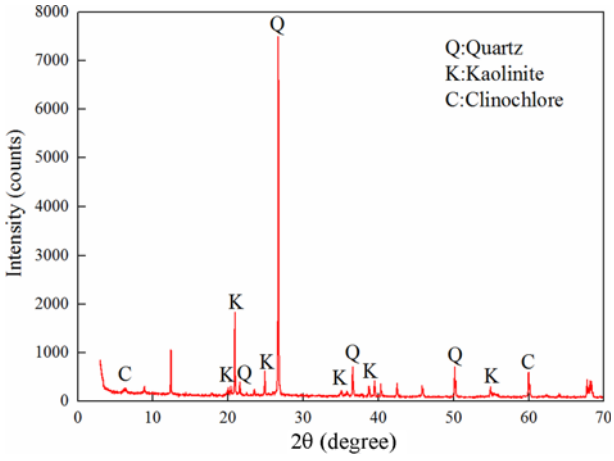


**Fig. 1.** XRD Patterns of the Sandstone

With the goal of producing accurate and credible results, the specimens were first selected so that there are no visible joints or cracks on each specimen's surface. Then the *P*-wave velocity of each specimen was tested. Finally, specimens with no visible joints or cracks, which have similar wave velocities were selected for the experiment. The specimens were divided into 6 groups corresponding to 6 different numbers of wetting-drying cycles. Each group contained 5 samples and a total of 30 specimens were prepared. The specimens prepared for the experiment were labelled as $n_x - l_r$, where $n_x$ is the number of cycles, and $l_r$ represents the loading rate.

### 2.2 Cyclic Wetting-Drying Process

Before the cyclic wetting-drying process, all the specimens were first dried for 24 h in an oven at 105°C to ensure that the rocks were fully dried. Generally, one cyclic wetting-drying could be separated into two stages: 1) the saturation stage (samples from a dry state to a saturated state) and 2) the drying stage (samples from a saturated state to a dry state), as shown in Fig. 2. During every cyclic wetting-drying, sandstone specimens were first immersed in purified water for 48 h in a container to ensure that the specimens would reach the water-saturated state, and then the specimens were removed and dried for 24 h in an oven at 105°C. In this study, sandstone specimens that do not experience cyclic wetting-dying are considered to undergo 0 cyclic wetting-drying process. In this experiment, a total number of 25 cyclic wetting-drying were performed. After every 5 cycles, the

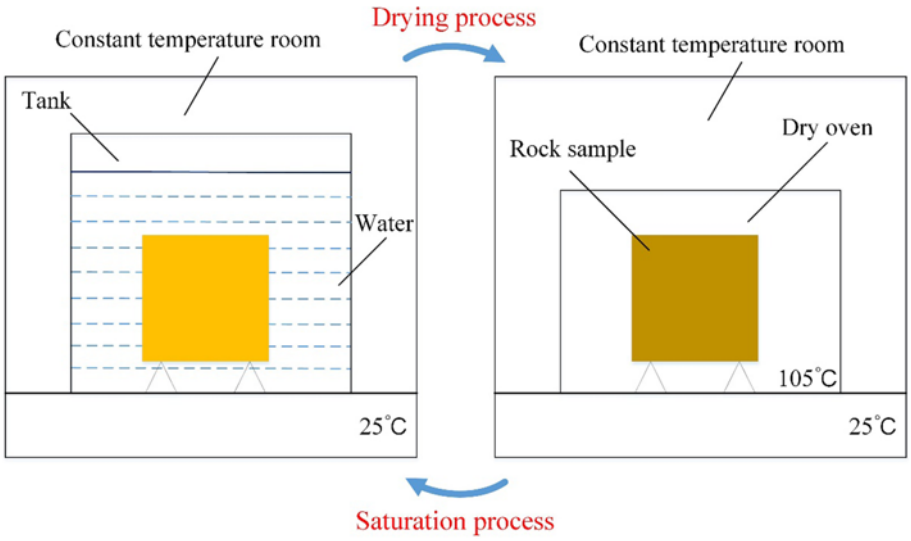


**Fig. 2.** Schematic Illustration of the Wetting-Drying Cycles

**Table 1.** Effect of Wetting-Drying Cycles on the Physical Properties of Sandstone

| Number of wetting-drying cycles | $\rho$/g·cm$^{-3}$ | | $w$/% | | $v_d$/10$^3$m·s$^{-1}$ | | $v_s$/10$^3$m·s$^{-1}$ | |
|---|---|---|---|---|---|---|---|---|
| | Average | SD | Average | SD | Average | SD | Average | SD |
| 0 | 2.224 | 0.004 | 4.006 | 0.142 | 3.032 | 0.019 | 3.203 | 0.012 |
| 5 | 2.197 | 0.001 | 4.341 | 0.069 | 2.720 | 0.012 | 3.131 | 0.015 |
| 10 | 2.191 | 0.002 | 4.444 | 0.121 | 2.607 | 0.009 | 3.040 | 0.011 |
| 15 | 2.185 | 0.004 | 4.631 | 0.054 | 2.522 | 0.011 | 2.951 | 0.021 |
| 20 | 2.181 | 0.002 | 4.679 | 0.123 | 2.461 | 0.009 | 2.901 | 0.009 |
| 25 | 2.177 | 0.07 | 4.696 | 0.023 | 2.425 | 0.013 | 2.875 | 0.014 |

Note: $\rho$ and $w$ represent density and water absorption of sandstone specimen, respectively; $v_d$ represents *P*-wave velocity of dry specimens and $v_s$ is that of water saturated specimens; SD denotes standard deviation.

physical, mechanical and AE parameters of the sandstone were determined. When the specific number of cycles was finished, the density and water absorption of each sample were first determined.

## 2.3 *P*-Wave Velocity

A nonmetallic acoustic testing system (RSM-SY6) was used to test the *P*-wave velocity of each sandstone specimen after every 5 cycles. To achieve good coupling between the specimens and probes, vaseline was applied onto the surface of the two probes before the testing process. The average wave velocity of the sandstone specimens in both dry state and saturated state can be found in Table 1.

## 2.4 Chemical Components Analysis of the Sandstone

The XRF technique was used to determine the chemical component variation of the specimens undergoing 0 and 25 cycles. To perform XRF, the sandstone specimens were first ground into powders finer than a 200 mesh. Then the test was conducted with S8 Tiger X-Ray Fluorite Spectroscopy.

## 2.5 SEM Test

To study the mechanism of different cyclic numbers on the rock's microstructure variations, the scanning electron microscope technique (SEM Quanta 250) was used to study the microscopic feature variations of sandstone samples undergoing 0, 5, 10, 15, 20 and 25 cycles.

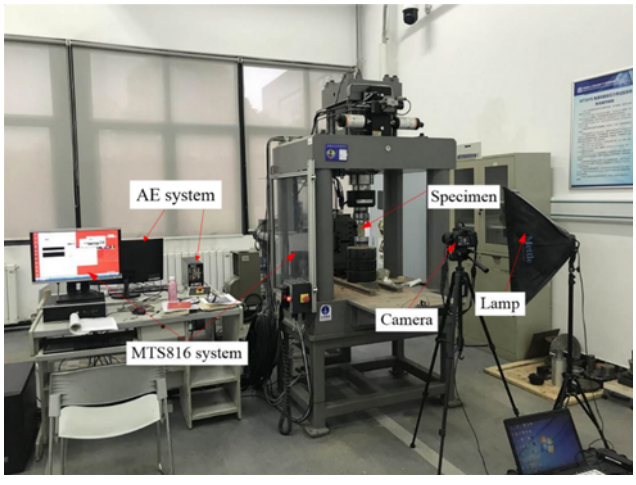


**Fig. 3.** MTS-816 Material Testing System

### 2.6 Uniaxial Compression Test

A MTS-816 electro-hydraulic servo mechanical testing system was employed to conduct the uniaxial compression test (shown in Fig. 3). The displacement loading mode was selected and the loading rate ($l_r$) was selected at 5 levels: 0.05, 0.1, 0.2, 0.4 and 0.8 mm/min. AE data were monitored and recorded during the whole test process. The crack evolution and damage process of each specimen were captured by a high resolution camera. Before the test began, petroleum jelly was smeared on the two ends of the specimen and the loading head to weaken the end effects.

## 3. Physical Properties of Sandstone Undergoing Wetting-Drying Cycles

First, physical property tests were performed on sandstone after every 5 cycles. The test results of the physical parameters are shown in Table 1.

### 3.1 Density

Figure 4 clearly shows the density variation of sandstone specimens undergoing different cycles. The results indicated that the density of sandstone would decrease with increasing cyclic numbers. After the sandstone specimens underwent 5, 10, 15, 20 and 25 cycles, the density was reduced by 1.20%, 1.49%, 1.76%, 1.94% and 2.13%, respectively. An exponential equation could be used to fit the relationship between the density and the cyclic numbers, and the best fitted line can be seen in Fig. 4.

### 3.2 Water Absorption

Figure 5 shows the variation tendency of water absorption with increasing cyclic numbers. It could be concluded that with increasing cyclic numbers, the water absorption would increase. When the number was 5, 10, 15, 20, and 25, the average water absorption increased by 8.36%, 10.92%, 15.59%, 16.78% and 17.20%, respectively. It can also be seen that an exponential equation could be used to fit the relationship between water absorption and cyclic numbers, and the best fitted line can be seen in Fig. 5.

### 3.3 *P*-Wave Velocity

It can be seen from Fig. 6 that under both the dry and saturated states, the *P*-wave velocity through the specimens would decrease with increasing cyclic numbers. This is because with increasing cyclic numbers, the porosity would increase and the density would decrease (Azimian and Ajalloeian, 2015; Kassab and Weller, 2015; Zhou et al., 2017). The exponential equation could be used to fit the relationship between the *P*-wave velocity and cyclic numbers. It can also be seen that the *P*-wave velocity in air was smaller than that in water. In the saturated state, air in the microcracks and voids was completely

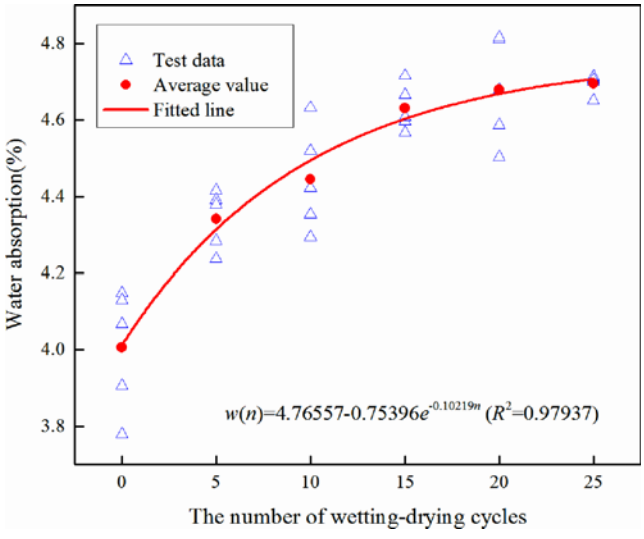


**Fig. 5.** Variation of Water Absorption versus Number of Wetting-Drying Cycles

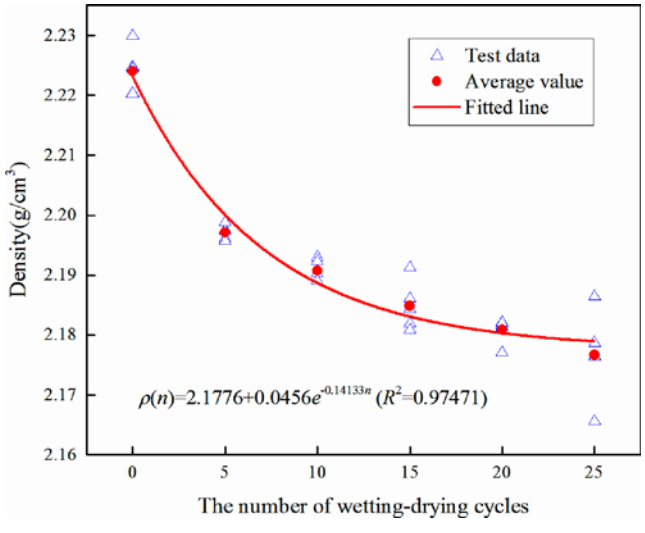


**Fig. 4.** Variation of Density versus Number of Wetting-Drying Cycles

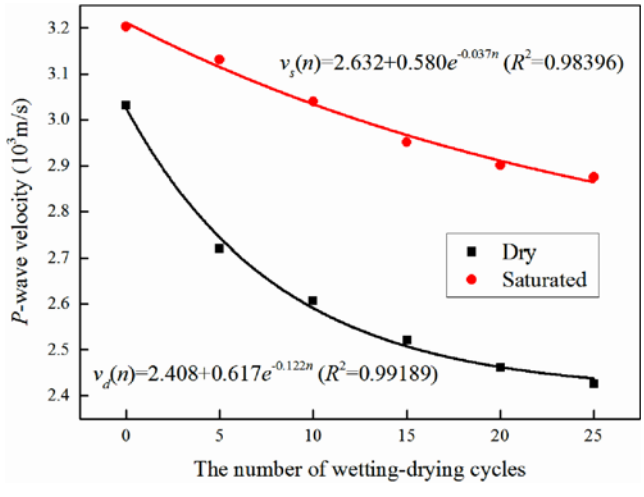


**Fig. 6.** Variation of *P*-Wave velocity versus Number of Wetting-Drying Cycles

**Table 2.** Quantitative Elemental Composition of the Specimens Undergoing 0 and 25 Wetting-Drying Cycles (%)

| The number of wetting-drying cycles | $Na_2O$ | MgO | $Al_2O_3$ | $SiO_2$ | $K_2O$ | CaO | $Fe_2O_3$ | Other |
|---|---|---|---|---|---|---|---|---|
| 0 | 0.07 | 0.31 | 17.81 | 75.89 | 1.11 | 0.14 | 4.06 | 0.61 |
| 25 | 0.07 | 0.37 | 17.16 | 75.60 | 1.26 | 0.12 | 4.62 | 0.80 |

replaced by water. Therefore, the reduction rate of sandstone's wave velocity under the saturated state was far less than that under the dry state.

## 4. Results of the XRF and SEM Analysis

Previous studies have proven that the microstructure and chemical components of rock can be altered during wetting-drying cycles. These alterations will lead to substantial attenuations of the rock properties. To understand the attenuation mechanism of wetting-drying cycles, XRF and SEM tests were conducted.

### 4.1 XRF Results

As shown in Table 2, the results demonstrate the following:

1. The specimens undergoing 0 and 25 wetting-drying cycles have the same chemical components. After 25 wetting-drying cycles, no new chemical components appeared, which means that chemical reactions did not occur between the sandstone specimen and water.
2. Sandstone specimens are mainly composed of $Fe_2O_3$, $Al_2O_3$ and $SiO_2$. The percentages of $Fe_2O_3$, $Al_2O_3$ and $SiO_2$ undergoing 0 wetting-drying cycles are 4.06%, 17.81% and 75.89% respectively. After 25 wetting-drying cycles, the percentages of $Fe_2O_3$, $Al_2O_3$ and $SiO_2$ are 4.06%, 17.81% and 75.89%, respectively. It can be observed that the difference in the three elements between the specimens after 0 and 25 cycles is very small.

The results presented that the effect of the wetting-drying cycles on the chemical components of the sandstone specimens can be ignored.

### 4.2 SEM Results

Figure 7 shows the SEM images (magnification ratio: 1,000) of the grain structures and micro-fractures after different cycles. Fig. 7(a) shows that the granules of the rock specimens are dense, and the selected original sample is intact, where microcracks are

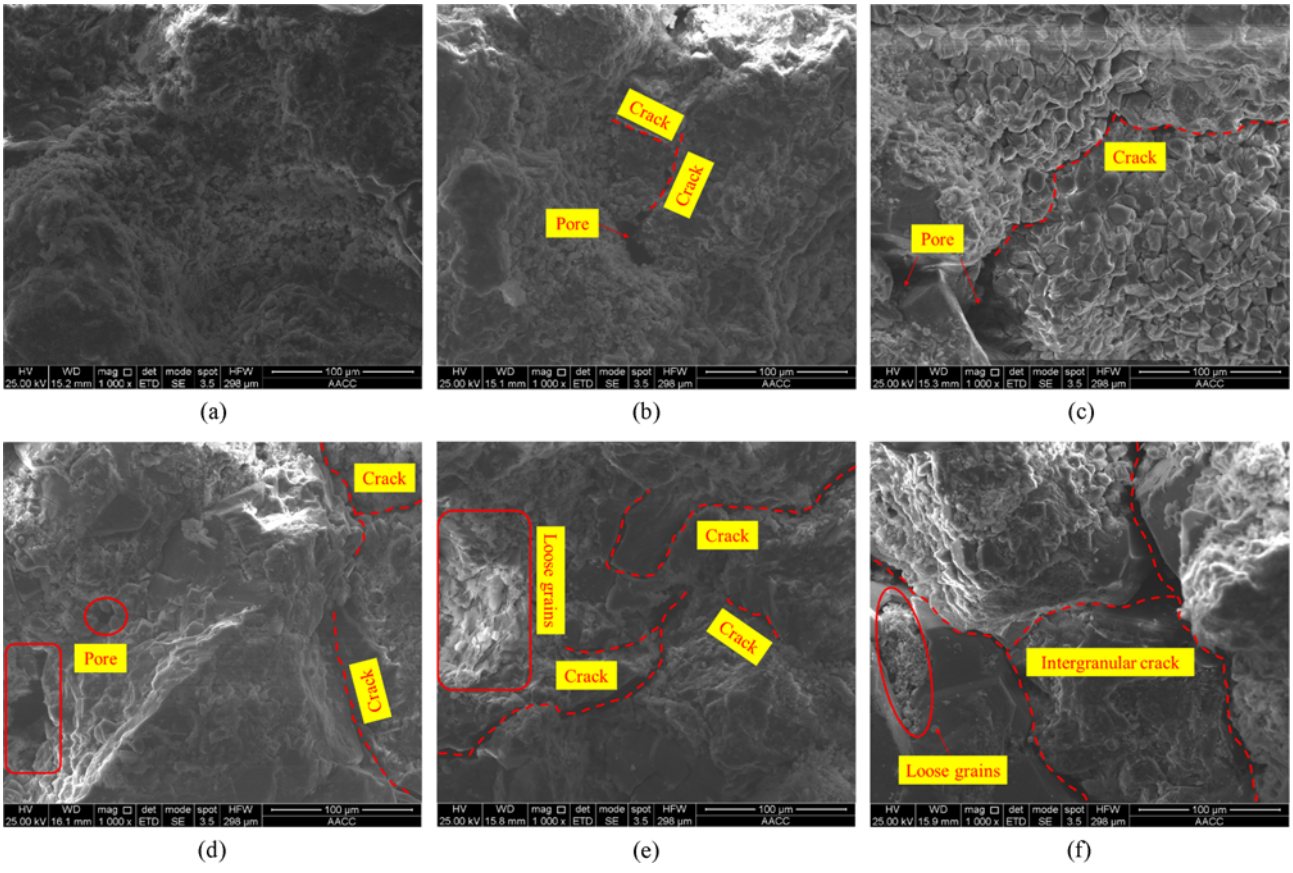


**Fig. 7.** SEM-Images for the Surfaces of Sandstone after Different Wetting-Drying Cycles: (a) n = 0, (b) n = 5, (c) n = 10, (d) n = 15, (e) n = 20, (f) n = 25

hardly visible. After the sample underwent 5 wetting-drying cycles, the grains become looser and newly formed microcracks can be discovered on the image (shown in Fig. 7(b)). This is because water in the rock causes crack initiation, propagation and coalescence. With increasing cyclic numbers, the damage to the rock would be aggravated. Therefore, both the quantity and width of the microcracks increase with increasing cyclic numbers. When the number reached 25, microcracks can almost be found between any sandstone grains, and the adjacent grains are almost separated (Fig. 7(f)). This observation indicates that wetting-drying cycles can lead to the microcrack growth and expansion in rocks.

From the XRF and SEM analysis, it can be concluded that the attenuation of rock properties undergoing wetting-drying cycles is mainly because of microcrack growth and expansion. Then the combination among the rock grains is weakened.

**Table 3.** Values of the UCS and $E$ of the Specimens after Wetting-Drying Cycles

| The number of wetting-drying cycles | $l_r$/mm·min$^{-1}$ | UCS/MPa | $E$/GPa |
|---|---|---|---|
| 0 | 0.05 | 60.85 | 9.15 |
| | 0.1 | 68.83 | 9.42 |
| | 0.2 | 74.23 | 10.07 |
| | 0.4 | 86.69 | 11.38 |
| | 0.8 | 90.84 | 12.44 |
| 5 | 0.05 | 48.22 | 7.67 |
| | 0.1 | 55.40 | 8.44 |
| | 0.2 | 60.33 | 9.11 |
| | 0.4 | 65.78 | 10.03 |
| | 0.8 | 70.22 | 10.80 |
| 10 | 0.05 | 41.02 | 6.92 |
| | 0.1 | 49.73 | 7.86 |
| | 0.2 | 53.09 | 8.32 |
| | 0.4 | 57.04 | 9.02 |
| | 0.8 | 64.18 | 9.61 |
| 15 | 0.05 | 36.87 | 6.58 |
| | 0.1 | 43.34 | 7.05 |
| | 0.2 | 48.24 | 7.64 |
| | 0.4 | 53.24 | 8.16 |
| | 0.8 | 59.50 | 8.66 |
| 20 | 0.05 | 31.09 | 6.32 |
| | 0.1 | 34.14 | 6.58 |
| | 0.2 | 39.67 | 7.01 |
| | 0.4 | 46.14 | 7.28 |
| | 0.8 | 52.74 | 7.81 |
| 25 | 0.05 | 25.40 | 5.90 |
| | 0.1 | 29.76 | 6.16 |
| | 0.2 | 34.59 | 6.35 |
| | 0.4 | 41.89 | 6.75 |
| | 0.8 | 46.56 | 7.23 |

## 5. Results of the Uniaxial Compression Test and AE Test

### 5.1 UCS and $E$

Table 3 shows the values of the UCS and $E$ after wetting-drying cycles. The changes in the UCS and $E$ of sandstone after each cyclic number can be separated into two stages (shown in Fig. 8). With increasing cyclic numbers, the UCS and $E$ gradually decrease. This is because the microcrack density increases and the combination among the rock grains is weakened with increasing cyclic number. The UCS and $E$ of sandstone after different cyclic numbers have the following characteristics:

1. The UCS of sandstone decreases with an increasing cyclic numbers. Before the number reaches 10, the uniaxial compressive strength decreases rapidly. When the number is greater than 10, the reduction in the UCS is less than that when the number is less than 10. For example, when the loading rate is 0.05 mm/min and the number of cycles increases from 0 to 10, the UCS decreases from 60.85 to

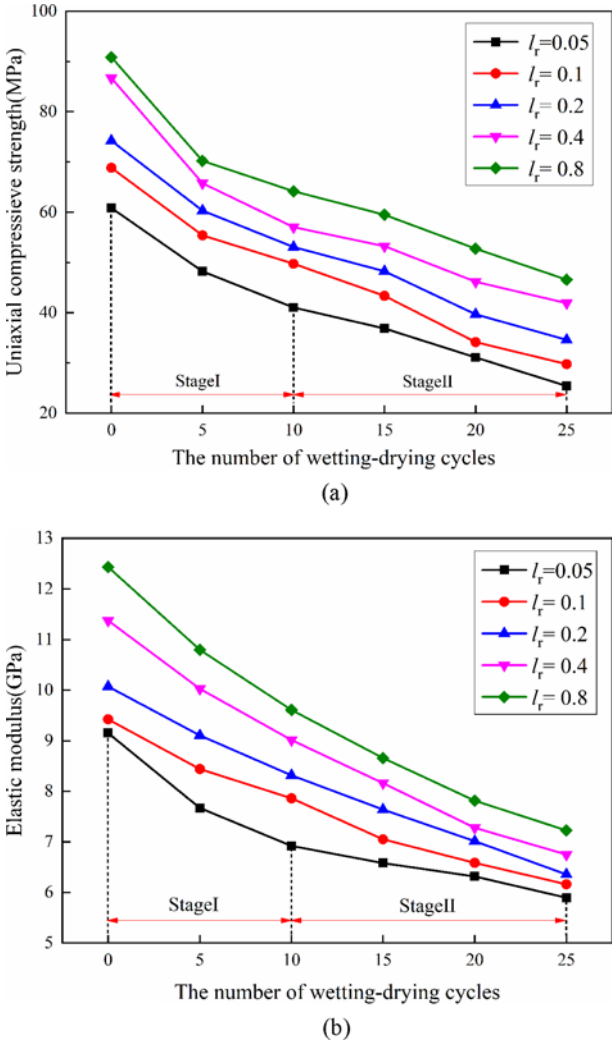


**Fig. 8.** Variations of the UCS and $E$ versus the Number of Wetting-Drying Cycles: (a) UCS, (b) $E$

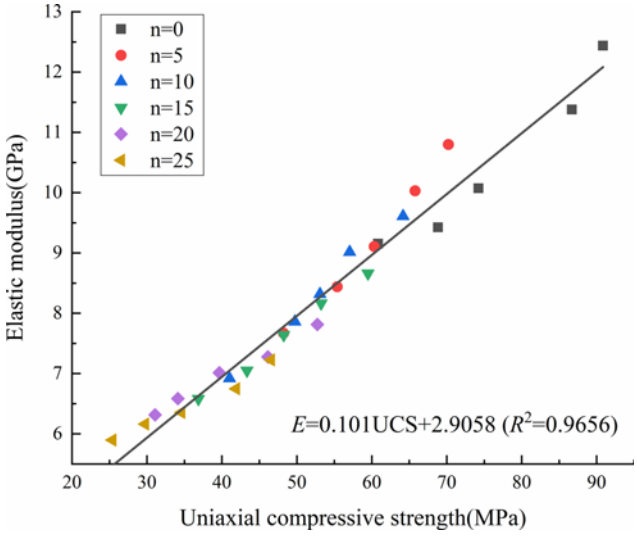


**Fig. 9.** The Relationship between UCS and *E*

41.02 MPa, with an average reduction rate of 16.30% after every 5 cycles. When the cyclic number increased to 25, the UCS decreases to 25.40 MPa, with an average reduction rate of 10.79% after every 5 cycles.

2. The *E* of sandstone decreases with an increasing cyclic numbers. Before the number reaches 10, *E* decreased rapidly.When the number is greater than 10, the reduction in *E* is less than that when the number is less than 10. For example, when the loading rate is 0.05 mm/min and the number of cycles increases from 0 to 10, *E* decreases from 9.15 to 6.92 GPa, with an average reduction rate of 12.20% after every 5 cycles. When the number of cycles increased to 25, *E* decreases to 5.90 GPa, with an average reduction rate of 4.93% after every 5 cycles.

Figure 9 shows the relationship between the UCS and *E* of sandstone undergoing different cyclic numbers. It can be seen that *E* has a nearly linear increase with increasing UCS. Therefore, the *E* of sandstone has a direct relation with the UCS.

## 5.2 AE Characteristics

Taking $l_r$ = 0.2 mm/min as an example, Fig. 10 shows the stress and AE counts evolutions of sandstone undergoing defferent cyclic numbers during the compression tests. The sandstone specimens undergoing defferent cyclic numbers showed some characteristics. The stress-time curve can be divided into four stages: the compaction stage, elastic stage, plastic stage and post peak stage. The compaction stage length increases with an increasing number of cycles. This is because with the increasing number of cycles, more microfissures will be generated inside the specimens. In the first two stages, very few AE counts will appear. Very obvious AE counts can be seen at the plastic stage and post peak stage. The maximum value of the AE counts can be observed very close to the peak stress.

To study the variation trends of the accumulated AE counts under different cyclic numbers, the accumulated AE counts-time curves are plotted as shown in Fig. 11. The relationship between the total AE counts and cyclic numbers was investigated (shown in Fig. 12). The accumulated AE counts curves of sandstone undergoing different cyclic numbers have a similar trend. At first, the curves of the accumulated AE counts increase very slowly with increasing time. Then, the curves of the accumulated AE counts increase sharply. Wetting-drying cycles cause damage to the sandstone specimens, and the damage degree of the sandstone specimens is aggravated as the cyclic numbers increase. Therefore, the rate of increase of the accumulated AE counts is reduced with an increasing cyclic number. As the cyclic number increases, the total AE counts of the sandstone decrease. From Table 4, it can be seen that the total AE counts of sandstone decrease almost linearly.

**Table 4.** Relationships between the Number of Wetting-Drying Cycles and the Total AE Counts

| $l_r$/mm·min$^{-1}$ | Relationship equation | $R^2$ |
|---|---|---|
| 0.05 | y = -0.1868n + 9.5197 | 0.8778 |
| 0.1 | y = -0.2198n + 15.694 | 0.8915 |
| 0.2 | y = -0.2511n + 18.749 | 0.9727 |
| 0.4 | y = -0.2666n + 22.328 | 0.926 |
| 0.8 | y = -0.29n + 28.083 | 0.9754 |

Note: y: the total AE counts

## 5.3 The Relationship between the AE and Mechanical Parameters

The relationships between the total AE counts and mechanical parameters (UCS and *E*) of sandstone after each cyclic number were analyzed and fitted as shown in Fig. 13. The UCS and *E* of sandstone after each cyclic number increased almost linearly with increasing total AE counts. Therefore, the mechanical parameters were directly related to the AE parameters. The UCS and *E* values of sandstone undergoing wetting-drying cycles could be predicted by the total AE counts. As a non-destructive testing method, AE testing could also be used as a promising method to record the AE signal of rock mass in actual engineering applications. Based on the AE data, the stress and deformation behavior of the rock mass could be precisely described using mathematical models (Vu-Bac et al., 2016; Samaniego et al., 2020). Then, the engineering safety and stability could be effectively ensured.

## 5.4 The Effect of the Loading Rates on the Mechanical and AE Characteristics

### 5.4.1 UCS and *E*

The changes in the mechanical parameters (UCS and *E*) under different loading rates are shown in Fig. 14. The relationship equations between the sandstone parameters and loading rate are fitted and shown in Table 5. The variations in the mechanical parameters under different loading rates show the following characteristics:

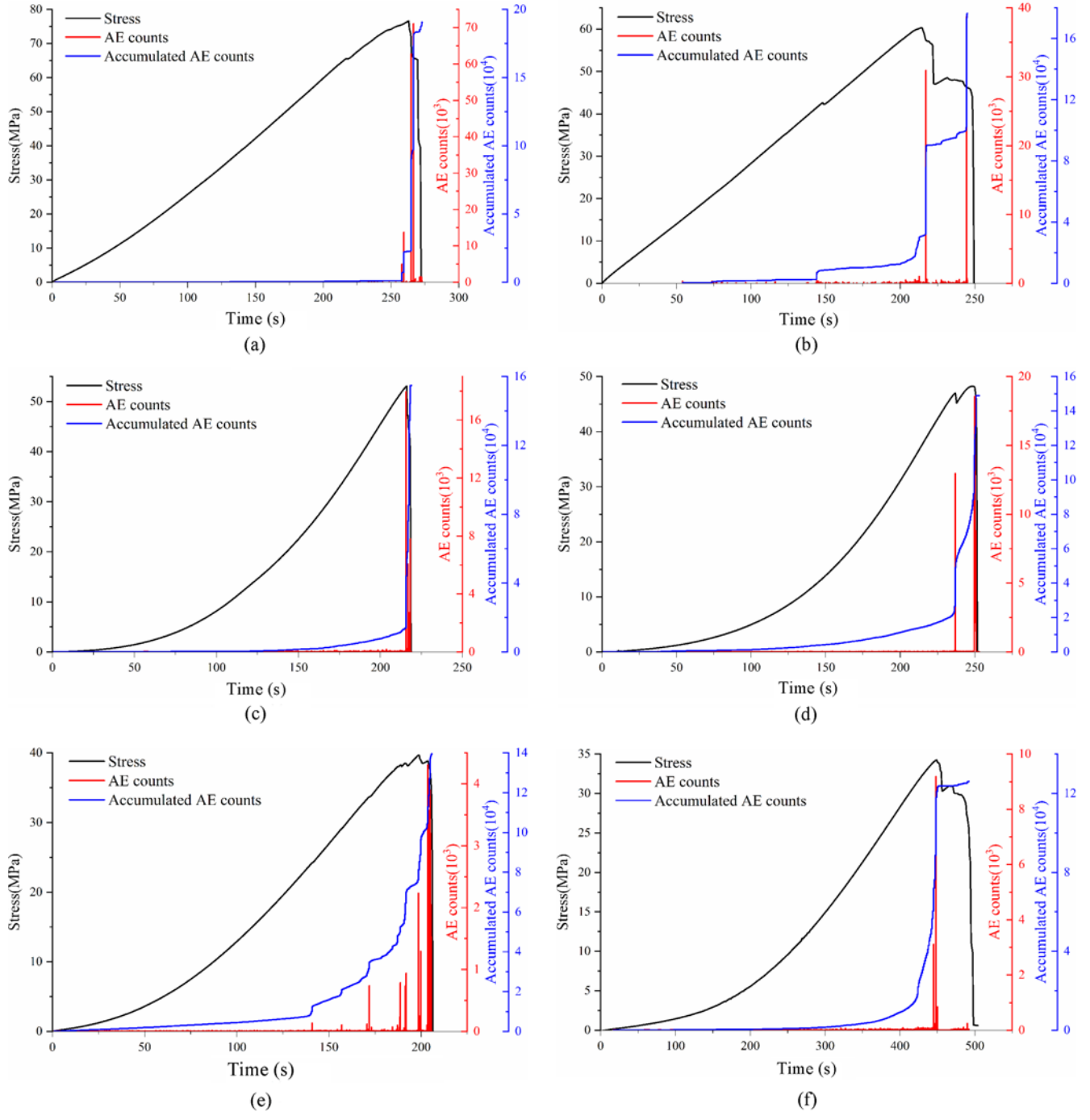


**Fig. 10.** Stress-Time-AE Counts Curves of Sandstone Undergoing Different Cyclic Numbers: (a) $n_0$-0.2, (b) $n_5$-0.2, (c) $n_{10}$-0.2, (d) $n_{15}$-0.2, (e) $n_{20}$-0.2, (f) $n_{25}$-0.2

1. With increasing loading rates, the UCS of sandstone after each cyclic number would increase. Taking n = 0 as an example, when the loading rate reached 0.8 mm/min from 0.05 mm/min, the UCS increased from 60.85 to 90.84 MPa, at a rate of 49.29%.
2. The *E* of sandstone after each cyclic number increased with increasing loading rate. For n = 0, when the loading rate reached 0.8 mm/min, *E* increased from 9.15 to 12.44 GPa, at a rate of 35.88%.
3. The relationship between the sandstone parameters (UCS and *E*) and loading rate could be matched by an exponential equation. With increasing loading rate, both the UCS and *E* would increase. The increasing rates of the UCS and *E* with increasing loading rate gradually decreased, and finally the UCS and *E* of the sandstone samples after different cyclic wetting-dryings tended to a constant value with increasing loading rate.

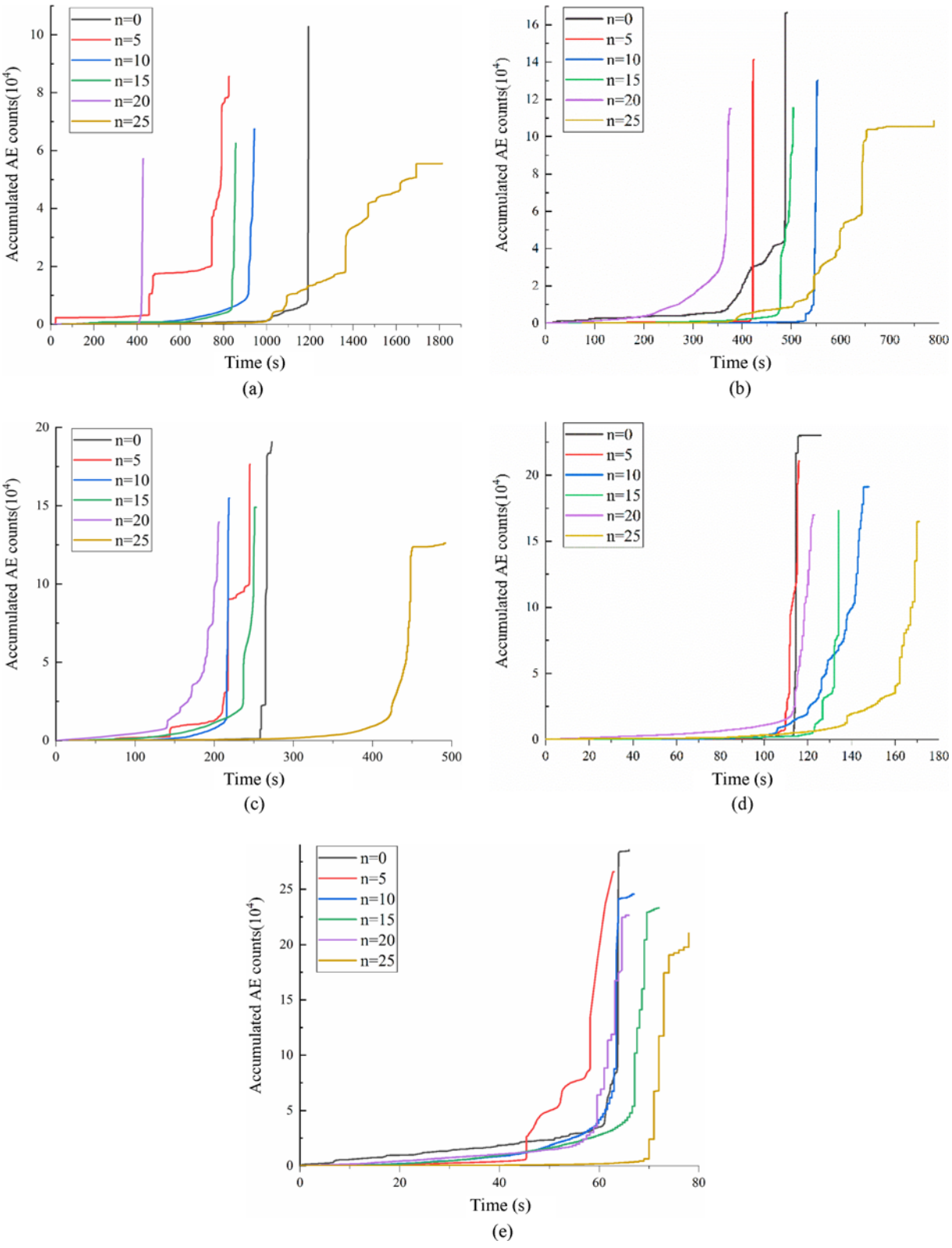


**Fig. 11.** Effect of Wetting-Drying Cycles on the Accumulated AE Counts of Sandstone: (a) $I_r$ = 0.05, (b) $I_r$ = 0.1, (c) $I_r$ = 0.2, (d) $I_r$ = 0.4, (e) $I_r$ = 0.8

### 5.4.2 AE Characteristics

The variations in the total AE counts of sandstone under different loading rates are shown in Fig. 15. With increasing loading rates, the total AE counts of sandstone after each cyclic number increase. The obtained conclusion is consistent with those of Zhang et al. (2017) and Backers et al. (2005). Taking n = 0 as an

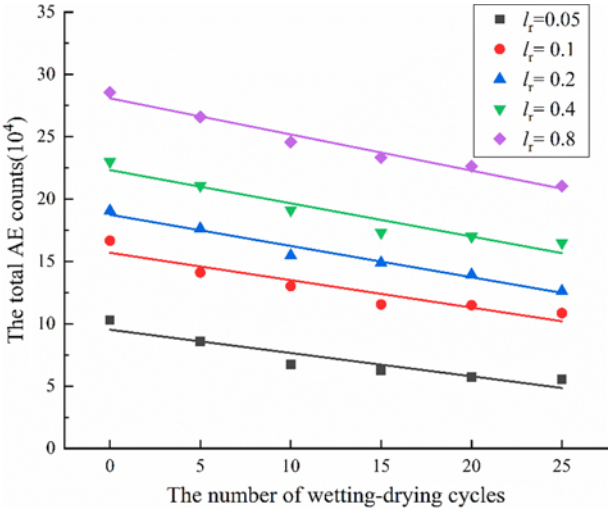


**Fig. 12.** Variations of the Total AE Counts versus Wetting-Drying Cycles

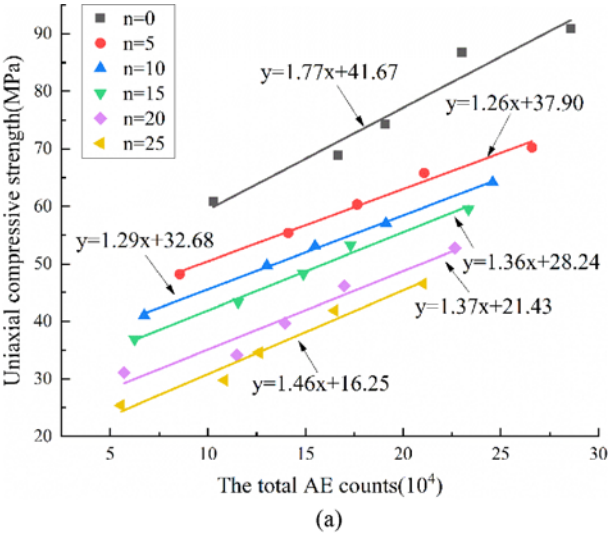


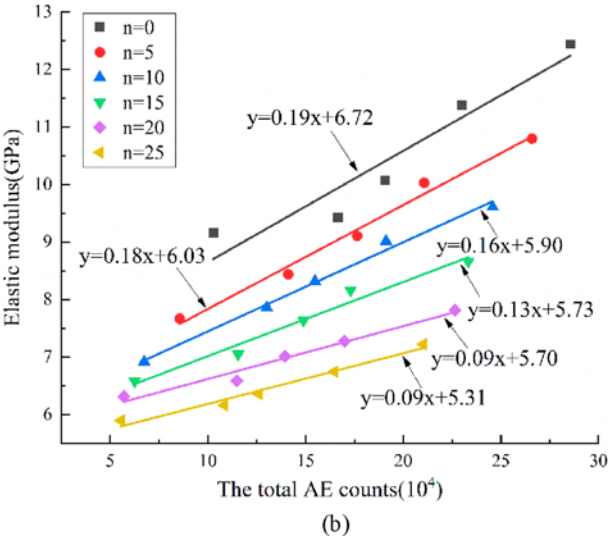


**Fig. 13.** Relationship between the Total AE Counts and Mechanical Parameters: (a) UCS, (b) *E*

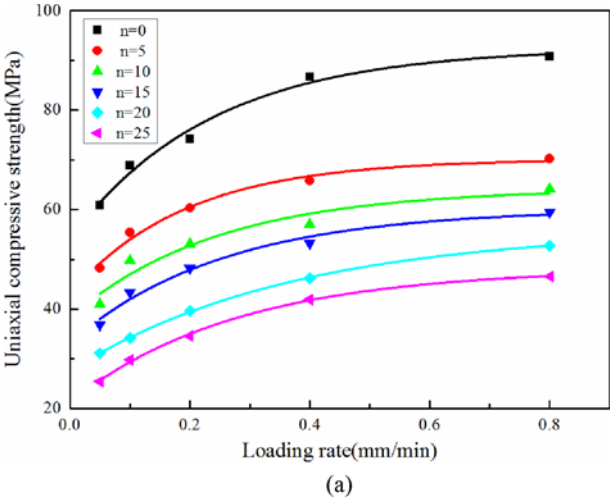


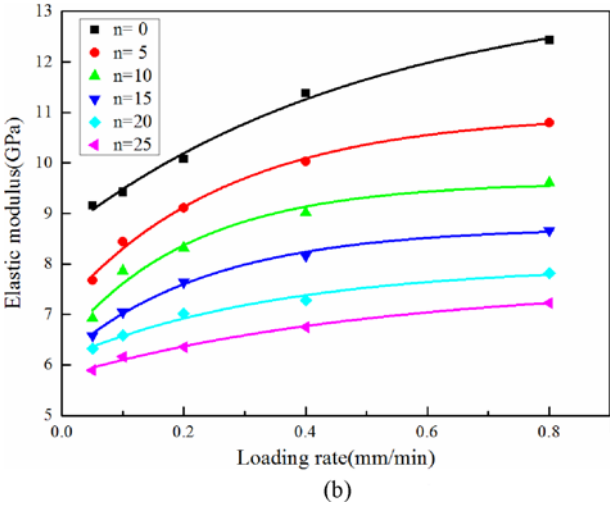


**Fig. 14.** Curve on the Change Relationship between the Sandstone Parameters and Loading Rate: (a) UCS, (b) *E*

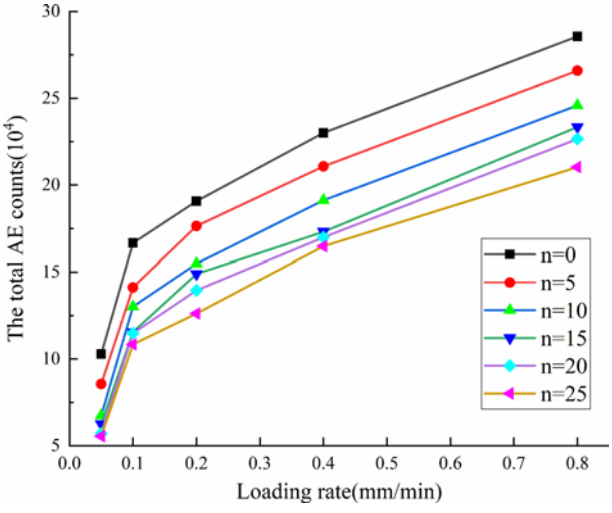


**Fig. 15.** Variations of the Total Number AE Counts versus Loading Rate

**Table 5.** Relationship Equations between the Sandstone Parameters and Loading Rate

| Parameters | The number of wetting-drying cycles | Relationship equation | $R^2$ |
|---|---|---|---|
| UCS | 0 | $UCS = 92.50316 - 38.53537e^{-4.25752l_r}$ | 0.97587 |
| | 5 | $UCS = 70.08999 - 27.20492e^{-5.21368l_r}$ | 0.97218 |
| | 10 | $UCS = 64.19071 - 25.98307e^{-4.09655l_r}$ | 0.88321 |
| | 15 | $UCS = 60.08004 - 26.95454e^{-3.9497l_r}$ | 0.96515 |
| | 20 | $UCS = 55.92322 - 28.43826e^{-2.71828l_r}$ | 0.99922 |
| | 25 | $UCS = 48.11961 - 26.9524e^{-3.59439l_r}$ | 0.99708 |
| $E$ | 0 | $E = 13.49113 - 4.87646e^{-1.95219l_r}$ | 0.98975 |
| | 5 | $E = 10.97423 - 3.86145e^{-3.68026l_r}$ | 0.98949 |
| | 10 | $E = 9.61447 - 3.21998e^{-4.74019l_r}$ | 0.95056 |
| | 15 | $E = 8.72183 - 2.59445e^{-4.18253l_r}$ | 0.99259 |
| | 20 | $E = 7.97841 - 1.86687e^{-2.82654l_r}$ | 0.96838 |
| | 25 | $E = 7.60545 - 1.83391e^{-1.95063l_r}$ | 0.98745 |

example, when the loading rate reaches 0.8 mm/min, the total AE counts increase from $10.28 \times 10^4$ to $28.56 \times 10^4$, at a rate of 178%.

## 6. Conclusions

In this paper, the effect of wetting-drying cycles on the physical, mechanical and AE characteristics of sandstone was studied. A series of physical parameters were first measured. After the physical tests, the effect of the loading rate on the mechanical and AE characteristics of rock undergoing wetting-drying cycles was experimentally studied using the MTS-816 electro-hydraulic servo test system and AE test system. The key findings can be drawn as follows:

1. This cyclic process would remarkably impact the physical properties of sandstone specimens. With an increasing number of cycles, the density and *P*-wave velocity would decrease, while the water absorption would increase. The relationship between the number of cycles and the physical parameters could be fitted by exponential equations.
2. By analysis the XRF results, it could be seen that chemical reactions did not occur between the sandstone specimens and water, and the difference in the three main chemical components between the specimens after 0 and 25 wetting-drying cycles was very small. From the SEM results, the process of wetting-drying cycles would lead to the microcrack initiation, generation and expansion inside the specimens. From the XRF and SEM analysis, it could be concluded that the attenuation of the rock properties undergoing wetting-drying cycles was mainly due to microcrack growth and expansion.
3. With an increasing cyclic numbers, both the UCS and *E* decrease. The accumulated AE counts curves of the sandstone undergoing different cyclic numbers first increase very slowly with increasing time. Then, the curves of the accumulated AE counts increase sharply. As the cyclic number increases, the rate of increase of the accumulated AE counts is reduced, and the total AE counts of the sandstone decrease almost linearly.
4. The functional relationships between the total AE counts and the mechanical parameters (UCS and *E*) of the sandstone after each cyclic number were established. Based on the functions, the UCS and *E* of sandstone undergoing a specific cyclic number could be predicted. This finding could be applied to the actual engineering applications to assess the mechanical characteristics of the rock mass under wetting-drying conditions.
5. As the loading rate increases, the UCS and *E* of sandstone at the same cyclic number increase. The relationship between the sandstone parameters (UCS and *E*) and loading rate can be matched by an exponential equation. With increasing loading rates, the total AE counts of the sandstone after each cyclic number increase.

## Acknowledgments

The financial supports from National Natural Science Foundation of China (Nos. 51734009 and 51904290) and Natural Science Foundation of Jiangsu Province, China (No. BK20180663) are gratefully acknowledged.

## ORCID

Not Applicable

## References

Azimian A, Ajalloeian R (2015) Empirical correlation of physical and mechanical properties of marly rocks with *P* wave velocity. *Arabian Journal of Geosciences* 8:1-11, DOI: 10.1007/s12517-013-1235-4

Backers T, Stanchits S, Dresen G (2005) Tensile fracture propagation and acoustic emission activity in sandstone: The effect of loading rate. *International Journal of Rock Mechanics and Mining Sciences*

42:1094-1101, DOI: 10.1016/j.ijrmms.2005.05.011

Cai X, Zhou ZL, Liu KW, Du XM, Zang HZ (2019) Water-weakening effects on the mechanical behavior of different rock types: Phenomena and mechanisms. *Applied Sciences-Basel* 9:1-18, DOI: 10.3390/app9204450

Deng HF, Li JL, Zhu M, Wang KW, Wang LH, Deng CJ (2012) Experimental research on strength deterioration rules of sandstone under "saturation-air dry" circulation function. *Rock and Soil Mechanics* 33(11):3306-3312, DOI: 10.16285/j.rsm.2012.11.015 (in Chinese)

Gong FQ, Yan JY, Luo S, Li XB (2019) Investigation on the linear energy storage and dissipation laws of rock materials under uniaxial compression. *Rock Mechanics and Rock Engineering* 54:4237-4255, DOI: 10.1007/s00603-019-01842-4

Hua W, Dong SM, Li YF, Wang QY (2016) Effect of cyclic wetting and drying on the pure mode II fracture toughness of sandstone. *Engineering Fracture Mechanics* 153:143-150, DOI: 10.1016/j.engfracmech.2015.11.020

Hua W, Dong SM, Li YF, Xu JG, Wang QY (2015) The influence of cyclic wetting and drying on the fracture toughness of sandstone. *International Journal of Rock Mechanics & Mining Sciences* 78:331-335, DOI: 10.1016/j.ijrmms.2015.06.010

Kassab MA, Weller A (2015) Study on *P*-wave and *S*-wave velocity in dry and wet sandstones of Tushka region. *Egyptian Journal of Petroleum* 28(1):1-11, DOI: 10.1016/j.ejpe.2015.02.001

Khanlari G, Abdilor Y (2015) Influence of wet-dry, freeze-thaw, and heat-cool cycles on the physical and mechanical properties of upper red sandstones in central Iran. *Bulletin of Engineering Geology and the Environment* 74:1287-1300, DOI: 10.1007/s10064-014-0691-8

Kim JS, Lee KS, Cho WJ, Choi HJ, Cho GC (2015) A comparative evaluation of stress-strain and acoustic emission methods for quantitative damage assessments of brittle rock. *Rock Mechanics and Rock Engineering* 48:495-508, DOI: 10.1007/s00603-014-0590-0

Lei RD, Wang Y, Zhang L, Liu BL, Long K, Luo P, Wang YK (2019) The evolution of sandstone microstructure and mechanical properties with thermal damage. *Energy Science & Engineering* 7(6):3058-3075, DOI: 10.1002/ese3.480

Liu XR, Jin MH, Li DL, Zhang L (2018) Strength deterioration of a Shaly sandstone under dry-wet cycles: A case study from the Three Gorges Reservoir in China. *Bulletin of Engineering Geology and the Environment* 77:1607-1621, DOI: 10.1007/s10064-017-1107-3

Liu PF, Liu XF, Tian GD, Gan F, Bi J (2020) Effect of thermal cycling and hydro-thermal cycling on physical and mechanical properties of sandstone. *Energy Science & Engineering* 8:718-730, DOI: 10.1002/ese3.544

Liu XR, Wang ZJ, Fu Y, Yuan W, Miao LL (2016) Macro/micro testing and damage and degradation of sandstones under dry-wet cycles. *Advances in Materials Science and Engineering* 2016:1-16, DOI: 10.1155/2016/7013032

Özbek A (2014) Investigation of the effects of wetting-drying and freezing-thawing cycles on some physical and mechanical properties of selected ignimbrites. *Bulletin of Engineering Geology and the Environment* 73:595-609, DOI: 10.1007/s10064-013-0519-y

Qin Z, Chen XX, Fu HL (2018) Damage features of altered rock subjected to drying-wetting cycles. *Advances in Civil Engineering* 2018:1-10, DOI: 10.1155/2018/5170832

Samaniego E, Anitescu C, Goswami S, Nguyen-Thanh VM, Guo H, Hamdia K, Zhuang X, Rabczuk T (2020) An energy approach to the solution of partial differential equations in computational mechanics via machine learning: Concepts, implementation and applications. *Computer Methods in Applied Mechanics and Engineering* 362(s1):1-29, DOI: 10.1016/j.cma.2019.112790

Sun Q, Zhang YL (2019) Combined effects of salt, cyclic wetting and drying cycles on the physical and mechanical properties of sandstone. *Engineering Geology* 248:70-79, DOI: 10.1016/j.enggeo.2018.11.009

Vu-Bac N, Lahmer T, Zhuang X, Nguyen-Thoi T, Rabczuk T (2016) A software framework for probabilistic sensitivity analysis for computationally expensive models. *Advances in Engineering Software* 100:19-31, DOI: 10.1016/j.advengsoft.2016.06.005

Wang JJ, Zhou YF, Wu X, Zhang HP (2019) Effects of soaking and cyclic wet-dry actions on shear strength of an artificially mixed sand. *KSCE Journal of Civil Engineering* 23(4):1617-1625, DOI: 10.1007/s12205-019-0896-2

Zhang ZH, Jiang QH, Zhou CB, Liu XT (2014) Strength and failure characteristics of Jurassic Red-Bed sandstone under cyclic wetting-drying conditions. *Geophysical Journal International* 198:1034-1044, DOI: 10.1093/gji/ggu181

Zhang BY, Zhang JH, Sun GL (2015) Deformation and shear strength of rockfill materials composed of soft siltstones subjected to stress, cyclical drying/wetting and temperature variations. *Engineering Geology* 190:87-97, DOI: 10.1016/j.enggeo.2015.03.006

Zhang XP, Zhang Q, Wu SC (2017) Acoustic emission characteristics of the rock-like material containing a single flaw under different compressive loading rates. *Computers and Geotechnics* 83:83-97, DOI: 10.1016/j.compgeo.2016.11.003

Zhao YF, Ren S, Jiang DY, Liu R, Wu JX, Jiang X (2018) Influence of wetting-drying cycles on the pore structure and mechanical properties of mudstone from Simian Mountain. *Construction and Building Materials* 191:923-931, DOI: 10.1016/j.conbuildmat.2018.10.069

Zhao ZH, Yang J, Zhang DF, Peng H (2017) Effects of wetting and cyclic wetting-drying on tensile strength of sandstone with a low clay mineral content. *Bulletin of Engineering Geology and the Environment* 50:485-491, DOI: 10.1007/s00603-016-1087-9

Zhou ZL, Cai X, Chen L, Cao WB, Zhao Y, Cheng X (2017) Influence of cyclic wetting and drying on physical and dynamic compressive properties of sandstone. *Engineering Geology* 220:1-12, DOI: 10.1016/j.enggeo.2017.01.017

Zhou ZL, Cai X, Ma D, Chen L, Wang SF, Tan LH (2018a) Dynamic tensile properties of sandstone subjected to wetting and drying cycles. *Construction and Building Materials* 182:215-232, DOI: 10.1016/j.conbuildmat.2018.06.056

Zhou SW, Zhuang XY (2020) Phase field modeling of hydraulic fracture propagation in transversely isotropic poroelastic media. *Acta Geotechnica* 15:2599-2618, DOI: 10.1007/s11440-020-00913-z

Zhou SW, Zhuang XY, Rabczuk T (2018b) A phase-field modeling approach of fracture propagation in poroelastic media. *Engineering Geology* 240:189-203, DOI: 10.1016/j.enggeo.2018.04.008

Zhou SW, Zhuang XY, Rabczuk T (2019) Phase-field modeling of fluid-driven dynamic cracking in porous media. *Computer Methods in Applied Mechanics and Engineering* 350:169-198, DOI: 10.1016/j.cma.2019.03.001

Zhou SW, Zhuang XY, Rabczuk T (2020) Phase field method for quasi-static hydro-fracture in porous media under stress boundary condition considering the effect of initial stress field. *Theoretical and Applied Fracture Mechanics* 107:1-15, DOI: 10.1016/j.tafmec.2020.102523

Zhuang XY, Zhou SW, Sheng M, Li GS (2020) On the hydraulic fracturing in naturally-layered porous media using the phase field method. *Engineering Geology* 266:1-16, DOI: 10.1016/j.enggeo.2019.105306